Lacassin & Mattauer 1985, NATURE

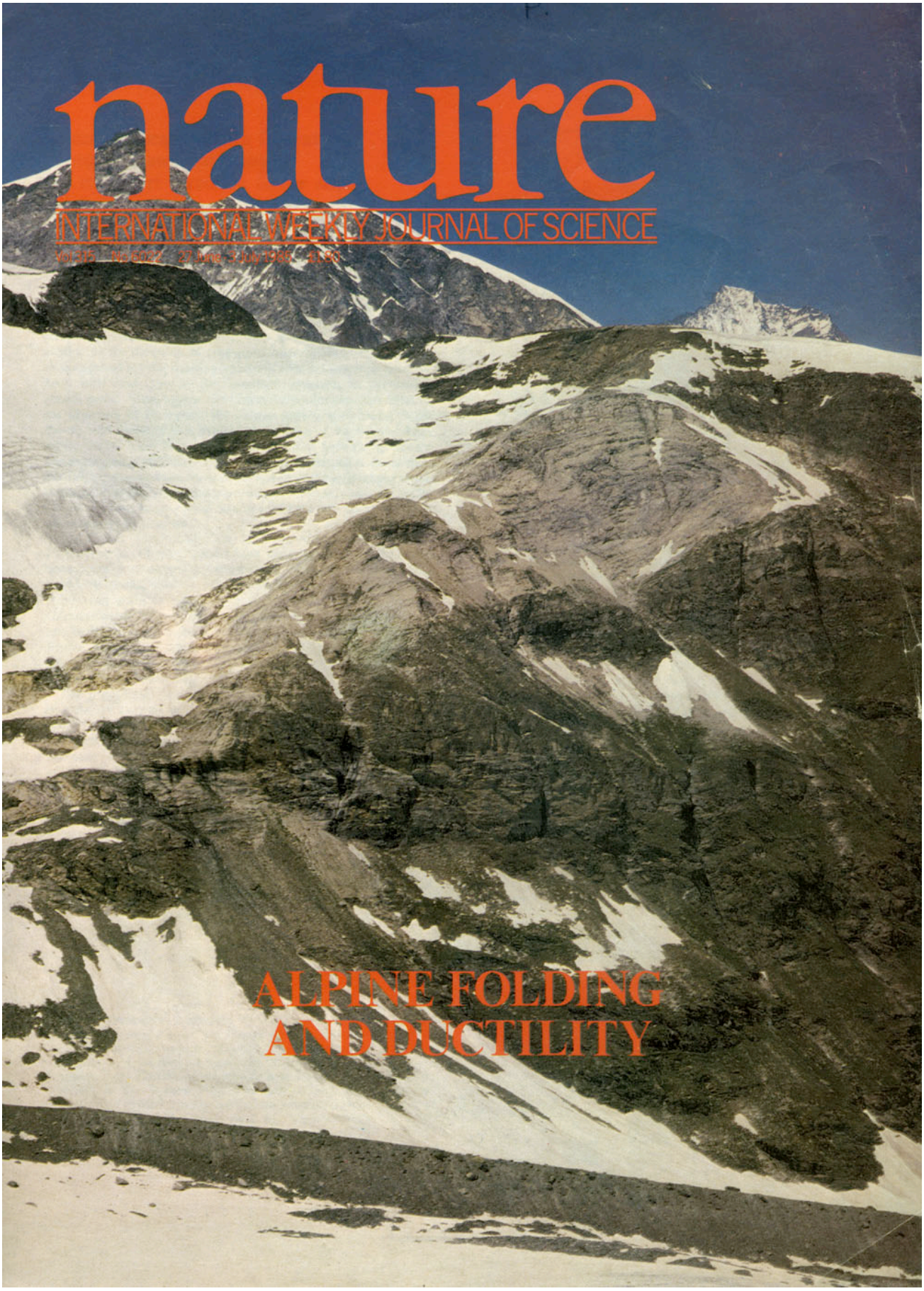

Reprinted from Nature, Vol. 316, No. 6022, pp. 739-742, 27 June 1985

Kilometre-scale sheath fold at Mattmark and implications for transport direction in the Alps

Robin Lacassin & Maurice Mattauer

Département des Sciences de la Terre, Université des Sciences et Techniques, Place E. Bataillon, 34060 Montpellier Cedex, France

Folds were the first tectonic features of rocks to be studied and as such are taken as a reference for the interpretation of other structures. Intuitively, fold axes were assumed to be subperpendicular to the direction of transport. Nevertheless, many studies of metamorphic belts showing intense ductile deformation describe folds with axes close to the transport direction. In particular, sheath folds[1–9], are highly curvilinear folds elongated parallel to the direction of transport. We discuss here a spectacular large sheath fold situated in a crustal shear zone in the Monte Rosa nappe, Swiss Alps. Our analysis implies that both the geometry and significance of folds in the internal Alps must be re-examined. We further demonstrate the existence of crustal ductile shear zones in an area of the Alps where previously emphasis was generally placed on fold nappes; the movements on these shear zones is often tens of kilometres.

The Monte Rosa nappe (Fig. 1), Swiss Alps, representing the northernmost internal crystalline massif, is a spectacular example of deep ductile deformation. It is made up of Hercynian basement rocks, mainly gneiss and schists, intruded by late Hercynian granites[10] and unconformably covered by Permo-Carboniferous volcaniclastic rocks and by a series of Mesozoic sediments[10–12]. All these were intensively reworked during the Alpine tectonometamorphism with the formation of gneisses, micaschists and mylonites, and are tectonically overlain by the Zermatt Saas-Fee ophiolite thrust sheet[13].

The polyphase Alpine metamorphism may be divided into two major events: as a high-pressure eoalpine metamorphism[14,15], (the climax of this metamorphism occurred around 110 Myr ago in eclogitic conditions (15 kbar), followed by a decrease of pressure to 7–8 kbar until 60 Myr)[16,17], and the Alpine (s.s.) metamorphism at around 38 Myr ago[17,18], in greenschist to amphibolite conditions.

In the Monte Rosa area, as in all the pennine Alps, the intensity of the Alpine deformation is evidenced by large recumbent nappes[19,20] and the presence of a prominent Alpine foliation and intense microfolding[10,21–23]. However, such studies can only analyse fold geometry and usually describe several phases of folding[24]. The direction of transport is generally assumed to be perpendicular to the fold axes and the vergence of 'tectonic phases' is deduced from the apparent vergence of folds.

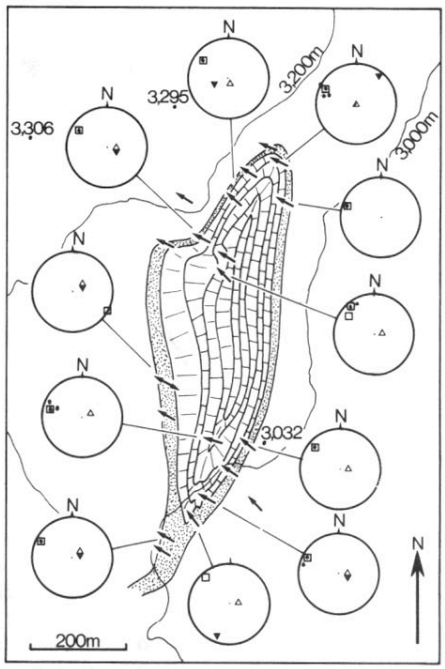

Fig. 2 Structural map of the 'eye fold'. The arrows represent the stretching lineations. In the Schmitt diagrams (lower hemisphere projection): △, foliation; ▲, stratification; □, stretching lineations; ●, intersection lineations (S_0/S_1 or S_0/S_{1-2}).

Our recent work[25,26] has attempted to study the deformation mechanisms using tectonic and microtectonic analysis. We obtained the following results: firstly, The most significant microstructure is the prominent stretching lineation. This is clearly recognized by the elongation of deformable markers (such as pebbles), the stretching of porphyroclasts or rigid inclusions (feldspars in gneissic rocks, dolomitic layer in marbles) and also by mineral elongation (biotite, phengite, recrystallized quartz, feldspar or calcite, elongation of pressure shadow crystallizations). These lineations represent finite extension. On average they trend N 110° E, plunging slightly to the west-north-west. Despite variations (from N 70° E to N 140° E) which may be related to heterogeneities of the deformation[27], they are regionally coherent. Secondly, the major deformation observed is generally intense and progressive, and shows evidence of non-coaxial deformation such as quartz petrofabrics[28], coherent displacement along shear zones[27],

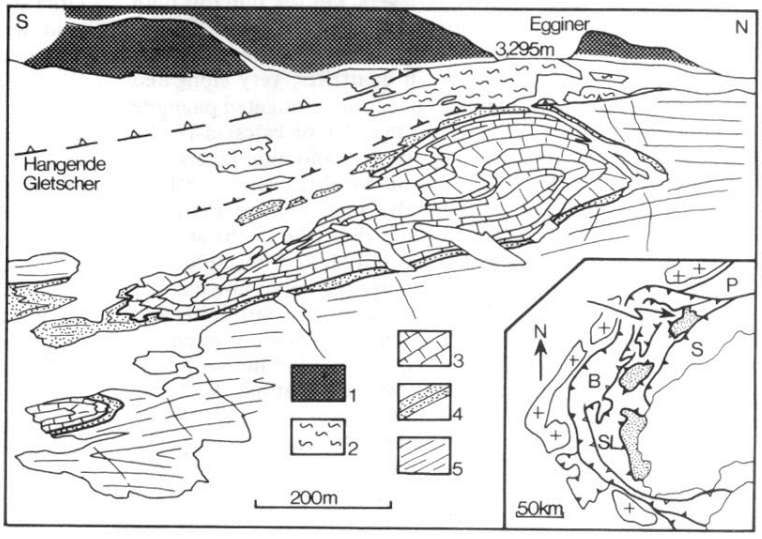

Fig. 1 Geological landscape of the 'eye fold' of Mattmark, viewed from the Gruenberghorn (3,015 m) towards the north-west. 1, Ophiolites; 2, Jurassic brown calcschists; 3, marbles; 4, quartzites; 5, paragneiss and schists. Inset location of the studied area (Monte Rosa nappe) in the Western Alps. The internal crystalline massifs are shaded; crosses indicate the external crystalline massifs. B, Briançonnais zone; SL, *Schistes lustrés* and ophiolites; S, Sesia zone; P, pennine nappes of the Lepontine area.

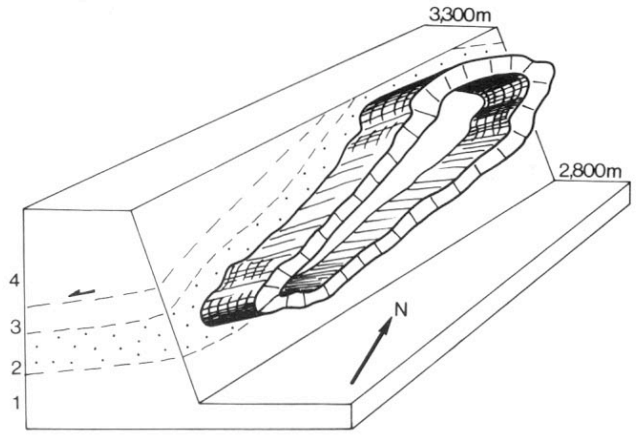

Fig. 3 Schematic structure of the 'eye fold'. 1, Paragneiss and schists; 2, quartzites; 3, calcschists; 4, ophiolitic thrust sheet (mainly serpentinites).

deformed porphyroclasts and pressure shadows[25], and shear band cleavages. Overall characteristics, the deformation resembles the result of simple shearing. As in shear zones the stretching lineation in the intensely deformed areas seems to lie close to the direction of shear.[29,30] On a regional scale, the lineations trace approximately straight paths. Two different units can be distinguished on the basis of the determined shear senses[25]. The first, the Monte Rosa nappe and its sedimentary cover, is characterized by shearing to the west-north-west associated with crustal ductile and major thrusting towards the west-north-west. The second unit, the Portjengrat unit, situated immediately south of the Mischabel backfold, shows east-south-eastward shears. We believe this deformation to be related to antithetic ductile thrusting[31]. Finally the observed progressive deformation mainly occurred during retrograde metamorphism at about 40 Myr. It may represent a late, although intense, phase of a complex deformation history and is probably related to major thrusting during and after continental collision.

In the vicinity of Mattmark in the Saas valley, a large-scale 'eye fold' has been recognized[32] and studied[25]. It is well exposed (Fig. 1), between 2,700 and 2,200 m, in a cliff oriented NNE-SSW and has been partly mapped[11,21]. It affects the sedimentary rocks of the Gornergrat zone with Upper Triassic marbles in the core of the fold, surrounded by Lower Triassic quartzites. This structure is in turn surrounded by schists and paragneisses (probably Permo-Carboniferous) and overlain by a slice of brown calcschists (*schistes lustrés* of supposed Jurassic age) and by the Zermatt Saas-Fee ophiolitic thrust sheet[13].

From the neighbouring summits (around 3,000 m) the 'eyed' structure is picked out by marble layers. On the outcrop both quartzite and marble layers surround the eye without discontinuity and define a closed structure (Fig. 1). The stretching lineation is generally prominent; in quartzites, very elongated pebbles, quartz rods and a mineral lineation (elongated phengite or quartz crystals) can be seen; in marbles or calcschists, the lineation is marked by boudinage of the dolomitic layers, the stretching of dolomitic inclusions or porphyroclasts (such as garnets) and elongation of minerals, and pressure shadows. These lineations show nearly constant direction in the studied area (Fig. 2) and on average trend N 120° E. Microfolds are isoclinal and more frequent in the north and south hinge zones of the eye fold (where we also observed small sheath folds and a mushroom-shaped fold) and also on the Jurassic calcschists. Both the fold axes (microfolds, north and south hinge zones of the eyed structure) and the intersection lineation, S_0/S_1 or S_0S_{1-2}, are parallel to the stretching lineation (Fig. 2).

The relative orientations of the bedding (S_0) and the fold axes suggest that the fold is cylindrical and that the eyed pattern is not a topographic effect (Fig. 3). Based on this structure and

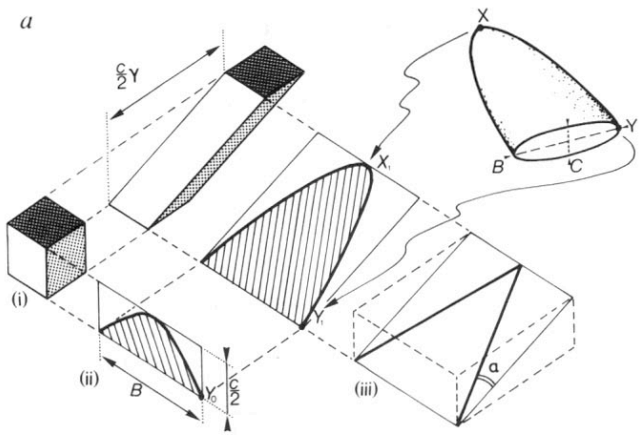

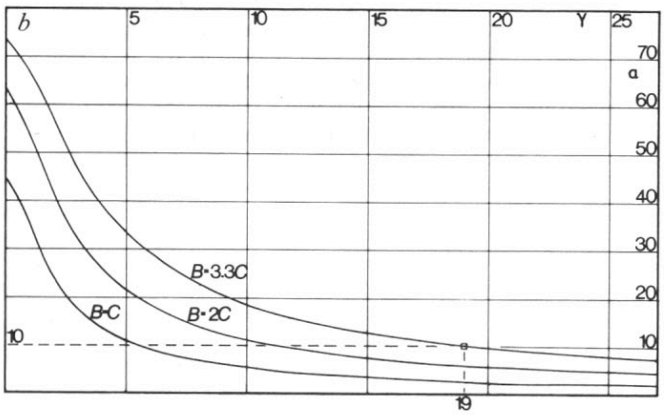

Fig. 4 Progressive reorientation of the limbs of a passive sheath fold. *a*, The model. (i) Idealized deformation of a cube of side. $C/2$ by simple shear (with shear strain γ); (ii) the same deformation applied to a cross-section of shape B, C representing the hinge zone of the fold; (iii) a simplification of this geometry to yield the angle α between the limbs and the long axis of the fold, as a function of γ and of the shape (B/C) of the fold. *b*, Curves of α versus γ. The curve $B = 3.3C$ corresponds to the fold of Mattmark. γ is estimated to a minimum value of 19.

on the intensity, mechanism and kinematic of deformation, we interpret this eye fold to be a section lying subperpendicular to the axis of a large sheath fold[1,2]. This fold would be elongated parallel to the stretching lineation trend and of the order of several kilometres in size. It represents a synclinal structure with the younger rocks (marbles) in the core. There is no direct evidence for an east or west closure of this fold, that is, an eastward- or westward-facing nose. It is possible that a such large sheath fold is the result of a dramatic deformation associated with the westward crustal shearing rather than ductile backthrusting; if this is the case, the closure of the synclinal sheath fold should be to the east.

Other large folds exist in the Gornegrat zone. For instance, immediately north of the eye fold, we have described a refolded isoclinal fold of kilometre scale whose axis is always parallel to the stretching lineation[25]. On the metric scale, most folds show certain characteristics consistently over the whole area studied: they are highly isoclinal with very elongated limbs; the fold axes are generally straight and parallel to the stretching lineation; folds are clearly visible in sections perpendicular to the lineation where their apparent vergence is generally to the south-west. Nevertheless, folds showing opposite vergence (both to the south and north) on the same outcrop and mushrooom-shaped folds are relatively common. Two major folding phases (F_1 and F_2) with the same geometrical characteristics have previously been described[22].

Hence, the present deformation analysis indicates that folds in the Monte Rosa area (except obvious late folds) may represent

either: (1) folds ("a folds")[33] with axes close to the long axis of the strain ellipsoid, as shown by the stretching lineation, which then approach the shear direction or (2) sheath folds; both result from or were strongly deformed during, the large progressive shearing.

The mechanism of formation of sheath folds during progressive deformation is well established[1,2]. They appear to be the result of kinematic amplification of 'deflections' in the folded layers which produced curvilinear folds that became progressively more elongated during the deformation. The presence of a kilometre-scale sheath fold suggests that the shearing mechanism took place over a large area and caused very large deformation and transport. Commonly occurring folds lying parallel to the direction of shear were probably formed by reorientation, during the progressive deformation, of folds initially lying oblique to the shear direction[30,34]. Such oblique folds may have been induced during this deformation by the shearing of layers inclined relative to the shear plane[35,36].

In the absence of strain markers, an estimate of the shear strain can be obtained from a simple model of the geometry and evolution of the sheath fold. If exact, such an estimate would be more significant than a point-by-point strain analysis, because it would represent the average bulk shear strain for the whole volume of rock.

Assuming simple shear for the progressive deformation (Fig. 4*a*(i)), and a passive sheath fold, the shape of the hinge zone (Fig. 4*a*(ii)), represented in Fig. 4*a*(iii) by a triangle, is considered to be the result of kinematic amplification[2] of the deflection (Fig. 4*a*(ii)). We may calculate the angle α as a function of the shape of the sheath fold (B/C) and the shear strain (γ):

$$\alpha = \arctan\left(\frac{B}{C}\,\frac{1}{\sqrt{\gamma^2+1}}\right) \qquad (1)$$

Different curves, for different values of B/C, can now be plotted (Fig. 4*b*); the curve $B/C = 10/3$ corresponds to the Mattmark fold. We may then relate the characteristics of the observed sheath fold (the angle between the fold axes in the two hinge zones of the eye, which corresponds to 2α). Based on the approximately cylindrical shape of the Mattmark fold, we can consider the angle between the two axes to be $<20°$ (that is, $\alpha \leqslant 10°$). This leads to a minimum estimate for the bulk shear strain of $\gamma = 19$, for a fold with the observed dimension ($B/C = 10/3$). Although this is an oversimplified model (which assumes simple shear, unknown shape of the deflection, and only passive reorientation), such an estimate may be a useful average value for the bulk shear strain. It agrees with the microstructural and textural characteristics of rocks such as: the elongation of quartz pebbles in conglomerates[25] (λ_1/λ_3 up to 50 and a K parameter close to 1 where λ_1 and λ_3 are finite strain axes and K is the shape parameter for the strain ellipsoid and is 1 when in plane strain); mylonitic microstructures[37]; and well-defined preferred lattice orientation of quartz.

In terms of transport, for a shear zone 1 km thick (minimum thickness for the intensely sheared area situated at the top of the Monte Rosa nappe), the value for γ obtained requires a minimum displacement of ~20 km. Note that much more movement may occur on discrete fault zones.

Such an analysis, associating folds with a deformation mechanism, has several implications.

First, for highly deformed areas, it seems logical to assume that folds perpendicular to transport ('b fold') cannot exist except in the case of late folds. This is true for mylonite zones[38] and also for deep parts of mountain belts such as the Himalayas[33], the Alps[39,40] or the North American Cordillera[41,42]. Hence, geometrical analyses of folds are not good kinematic indicators and must be used in association with analyses of ductile deformation mechanisms.

Second, this work demonstrates the importance of thrust displacements of several tens of kilometres along ductile shear zones, in an area where previously much emphasis was placed on fold nappes[19,22–24]. As has already been proposed for the French–Italian Alps[40], deformation analyses show that the evolution of the Swiss part of the belt is highly logical, and is dominated by thrusting towards the west-north-west, without major gaps between the external and internal Alps.

Finally, deformation analysis should be carried out on all the internal parts of the Alps. Some advances have been made on the French–Italian part[43,44], but in the famous Pennine nappes of the Swiss Alps[19,20] studies have concentrated on the superposed folding[23,24,45]. According to the highly deformed state of the rocks, fold geometry seems to be unrelated to the kinematic evolution, except in the case of late folds. It is probable that major deformations occurred in a shear context[46,47] with the formation of stretching lineations[48,49] tracing the shear directions. It would now be of great interest to study ductile deformation and its kinematics and to relate it to the fold geometries, with a view to analysing sheath folds[47] and folds subparallel to the shear directions.

We thank P. Cobbold, A. Etchecopar, J. Malavieille, P. Tapponnier and J. Van Den Driessche for constructive criticism and discussions. This work was supported by the ATP Géodvnamique of CNRS–INAG and by the LA266–CNRS.

Received 21 January; accepted 3 May 1985.

1. Quinquis, H., Audren, C., Brun, J. P. & Cobbold, P. *Nature* **273,** 43–45 (1978).
2. Cobbold, P. & Quinquis, H. *J. struct. Geol.* **2,** 119–126 (1980).
3. Carreras, J., Estrada, A. & White, S. *Tectonophysics* **39,** 3–24 (1977).
4. Rhodes, S. & Gayer, R. A. *Geol. Mag.* **114,** 329–361 (1977).
5. Minnigh, L. *J. struct. Geol.* **1,** 275–282 (1979).
6. Talbot, C. J. *J. struct. Geol.* **1,** 5–18 (1979).
7. Faure, M. & Malavieille, J. *C.r. hebd. Séanc. Acad. Sci., Paris* D**290,** 1349–1352 (1980).
8. Carpéna, J. & Mailhé, D. *C.r. hebd. Séanc. Acad. Sci., Paris.* **298,** 415–418 (1984).
9. Henderson, J. *J. struct. Geol.* **3,** 203–210 (1981).
10. Bearth, P. *Beitr. geol. Karte Schweiz* **96,** (1952).
11. Guller, A. *Eclog. geol. Helv.* **40,** 41–151 (1947).
12. Bearth, P. *Eclog. geol. Helv.* **69,** 149–161 (1976).
13. Bearth, P. *Beitr. geol. Karte Schweiz* **132,** (1967).
14. Kiénast, J. R. *C.r. hebd. Séanc. Acad. Sci., Paris* D**276,** 2621–2624 (1973).
15. Ernst, N. & Dal Piaz, G. *Am. Miner.* **63,** 621–640 (1978).
16. Chopin, C. & Monié, P. *Contr. Miner. Petrol.* **87,** 388–398 (1984).
17. Monié, P. thesis, Univ. Montpellier (1984).
18. Hunziker, J. C. *Eclog. geol. Helv.* **63,** 151–161 (1970).
19. Argand, E. *Beitr. geol. Karte Schweiz* **31,** 1–26 (1911).
20. Homewood, P., Gosso, G., Escher, A. & Milnes, A. G. *Eclog. geol. Helv.* **73,** 635–643 (1980).
21. Bearth, P. *Atlas Géol. Suise Saas and Monte Moro* (Schweiz. Geol. Kommission, Basel, 1957).
22. Klein, J. A. *Leid. geol. Meded.* **51,** 233–312 (1978).
23. Muller, R. *Eclog. geol. Helv.* **76,** 391–416 (1983).
24. Milnes, A. G., Greller, M. & Muller, R. *J. struct. Geol.* **3,** 411–420 (1981).
25. Lacassin, R. thesis, Univ. Montpellier (1984).
26. Lacassin, R. *Tectonics* (submitted).
27. Lacassin, R. *C.r. hebd. Séanc. Acad. Sci., Paris* **296,** 777–782 (1983).
28. Lacassin, R. *C.r. hebd. Séanc. Acad. Sci., Paris* **297,** 613–618 (1983).
29. Ramsay, J. G. & Graham, R. *Can. J. Earth Sci.* **7,** 786–812 (1970).
30. Escher, A. & Watterson, J. *Tectonophysics* **22,** 223–231 (1974).
31. Malavieille, J. *Bull. Soc. géol. Fr.* **26,** 129–138 (1984).
32. Mattauer, M. *C.r. hebd. Séanc. Acad. Sci., Paris* **293,** 929–932 (1981).
33. Mattauer, M. *Earth planet. Sci. Lett.* **28,** 144–154 (1975).
34. Sanderson, D. *Tectonophysics* **16,** 55–70 (1973).
35. Berthé, D. & Brun, J. P. *J. struct. Geol.* **2,** 127–133 (1980).
36. Hugon, H. thesis, Univ. Rennes (1982).
37. White, S., Burrows, S., Carreras, J., Shaw, N. & Humphreys, F. *J. struct. Geol.* **2,** 175–187 (1980).
38. Hobbs, B., Means, W. & Williams, P. *An Outline of Structural Geology* (Wiley, New York, 1976).
39. Nicolas, A. & Boudier, F. *Tectonophysics* **25,** 233–260 (1975).
40. Malavieille, J., Lacassin, R. & Mattauer, M. *Bull. Soc. géol. Fr.* **26,** 895–906 (1984).
41. Mattauer, M., Faure, M. & Malavieille, J. *J. struct. Geol.* **3,** 401–409 (1981).
42. Van Den Driessche, J. *Tectonophysics* (in the press).
43. Laurent, P. & Etchecopar, A. *Bull. Soc. géol. Fr.* **18,** 1387–1393 (1976).
44. Malavieille, J. & Etchecopar, A. *Tectonophysics* **78,** 65–71 (1981).
45. Hubert, M., Ramsay, J. G. & Simpson, C. *Eclog. geol. Helv.* **73,** 593–607 (1980).
46. Simpson, C. *Eclog. geol. Helv.* **75,** 495–516 (1982).
47. Cobbold P. *J. struct. Geol.* **1,** 338 (1979).
48. Steck, A. *Bull. geol. Lausanne* 252 (1980).
49. Steck, A. *Eclog. geol. Helv.* **77,** 55–100 (1984).